JACS
JOURNAL OF THE AMERICAN CHEMICAL SOCIETY

ARTICLE

pubs.acs.org/JACS

Unified Molecular View of the Air/Water Interface Based on Experimental and Theoretical $\chi^{(2)}$ Spectra of an Isotopically Diluted Water Surface

Satoshi Nihonyanagi,[†] Tatsuya Ishiyama,[‡] Touk-kwan Lee,[‡] Shoichi Yamaguchi,[†] Mischa Bonn,[§,∥] Akihiro Morita,[*,‡] and Tahei Tahara[*,†]

[†]Molecular Spectroscopy Laboratory, Advanced Science Institute, RIKEN, 2-1 Hirosawa, Wako, Saitama 351-0198, Japan

[‡]Department of Chemistry, Graduate School of Science, Tohoku University, Sendai 980-8578, Japan

[§]Max Planck Institute for Polymer Research, Ackermannweg 10, 55128 Mainz, Germany

[∥]FOM-Institute AMOLF, Science Park 104, 1098 XG Amsterdam, The Netherlands

Supporting Information Web-Enhanced

ABSTRACT: The energetically unfavorable termination of the hydrogen-bonded network of water molecules at the air/water interface causes molecular rearrangement to minimize the free energy. The long-standing question is *how water minimizes the surface free energy*. The combination of advanced, surface-specific nonlinear spectroscopy and theoretical simulation provides new insights. The complex $\chi^{(2)}$ spectra of isotopically diluted water surfaces obtained by heterodyne-detected sum frequency generation spectroscopy and molecular dynamics simulation show excellent agreement, assuring the validity of the microscopic picture given in the simulation. The present study indicates that there is no ice-like structure at the surface—in other words, there is no increase of tetrahedrally coordinated structure compared to the bulk—but that there are water pairs interacting with a strong hydrogen bond at the outermost surface. Intuitively, this can be considered a consequence of the lack of a hydrogen bond toward the upper gas phase, enhancing the lateral interaction at the boundary. This study also confirms that the major source of the isotope effect on the water $\chi^{(2)}$ spectra is the intramolecular anharmonic coupling, i.e., Fermi resonance.

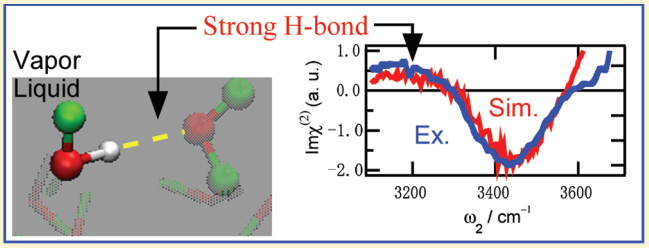

1. INTRODUCTION

Understanding the structure of the pure water surface is of essential importance in fundamental science. As a result of the truncation of the hydrogen bond network, the structure of the water surface must differ from that in the bulk. However, the molecular structure of the water surface is still strongly debated, as it has been for the bulk.[1−6] An interface-selective spectroscopy, vibrational sum frequency generation (VSFG), pioneered by Shen and co-workers, has been widely utilized to study aqueous interfaces with vibrational spectroscopy.[7−10] The VSFG spectrum of the neat water surface shows two broad OH bands around 3200 cm^{-1} (OH(I)) and 3400 cm^{-1} (OH(II)), in addition to a sharp OH band due to "free" OH at 3700 cm^{-1}. Because the two broad bands resemble the infrared OH stretch bands of the ice and liquid water in bulk, Shen and co-workers called the two bands "ice-like" and "liquid-like" bands.[8,11,12] They assigned the ice-like band to tetrahedrally coordinated water[11,12] and concluded that "the water surface has a partially disordered icelike structure".[8]

Recently, however, Bonn and co-workers showed that the two peaks in the VSFG spectrum of the neat water surface merge upon isotopic dilution and suggested that they are not associated with two distinct structures but arise from intramolecular coupling of the HOH (DOD) vibrations.[13,14] In these conventional VSFG studies, the absolute square of the second-order nonlinear susceptibility ($|\chi^{(2)}|^2$) was measured, but the complex $\chi^{(2)}$ spectrum is much more informative and can be directly measured by phase-sensitive[15,16] or heterodyne-detected VSFG (HD-VSFG)[17−23] techniques. Tian and Shen measured Im$\chi^{(2)}$ spectra of isotopically diluted water surfaces, in which the intramolecular coupling is eliminated, and they found that a positive band (∼3300 cm^{-1}, OH(x)) and a negative band (∼3480 cm^{-1}, OH(0)) appear in the OH stretch region, even though the $|\chi^{(2)}|^2$ spectrum shows only a single band.[24,25] Tian and Shen attributed the positive OH(x) band to ice-like symmetric tetrahedrally H-bonded water molecules and the negative OH(0) band to "liquid-like" water at the air/water interface.[24]

The appearance of the low-frequency OH(x) band implies the presence of stronger H-bonds at the surface, but it does not necessarily originate from the tetrahedral "ice-like" structure. Indeed, previous theoretical studies have proposed various

Received: June 10, 2011
Published: September 07, 2011

dx.doi.org/10.1021/ja2053754 | J. Am. Chem. Soc. 2011, 133, 16875–16880

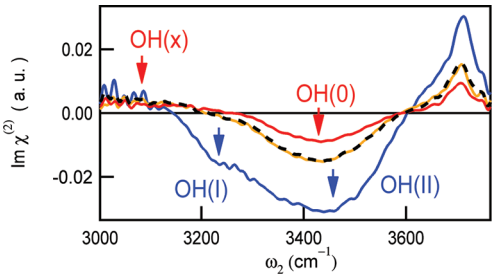

Figure 1. Im$\chi^{(2)}$ spectra of air/water interfaces with various isotope concentrations (blue, neat H_2O; dark yellow, H_2O:HOD:D_2O = 2:5:3; red, H_2O:OD:D_2O = 1:6:9). The sum frequency, visible, and infrared beams were s-, s-, and p-polarized, respectively. The black dashed line shows the linear combination of the Im$\chi^{(2)}$ spectra of the water with highest and lowest deuterium concentrations.

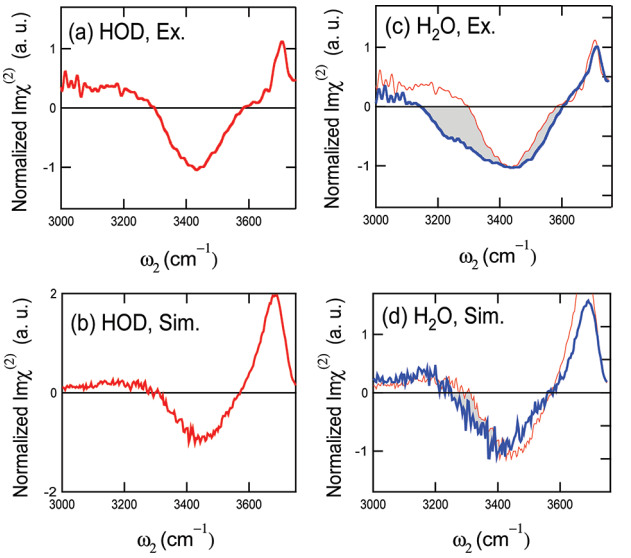

Figure 2. Intensity-normalized Im$\chi^{(2)}$ spectra of water surfaces. (a) Experimental HOD (red line), (b) simulated HOD (red), (c) experimental H_2O (blue), and (d) simulated H_2O (blue). In (c), the experimental HOD spectrum (a) is also shown by a thin red line. The shaded area represents the broadening of the negative OH band in H_2O spectra. In (d), spectrum (b) is also shown in a similar manner.

reasons other than the tetrahedral structure to explain the origin of the low-frequency OH(x) band.[9,26−30] In particular, Ishiyama and Morita calculated Im$\chi^{(2)}$ spectra of the air/H_2O interface based on a flexible and polarizable MD simulation and associated the OH(x) band to a pair of strongly H-bonded water molecules present at the outermost surface.[28−30] However, their calculated Im$\chi^{(2)}$ spectrum for the H_2O water surface cannot directly be compared with the experimental spectrum, because the classical MD simulation does not adequately take account of the Fermi resonance. Therefore, to clarify the structure of the air/water interface and to solve the debate, it is critically important to compare the simulated Im$\chi^{(2)}$ spectrum of the HOD surface with the experimental spectrum that is free from the effects of intra-/intermolecular coupling.

The aim of the present study is to present a unified view of the molecular structure at the water surface based on a combination of advanced experiment and theory. To achieve this, we carried out multiplex HD-VSFG measurements of the HOD water surface which provides complex $\chi^{(2)}$ spectra with a high phase stability, a large number of spectral data points, and an improved signal-to-noise ratio compared to single-channel phase-sensitive detection. Simultaneously, a new MD simulation was performed for HOD molecules to directly compare the experimental and theoretical Im$\chi^{(2)}$ spectra without the influence of intramolecular coupling. The excellent agreement between experiment and theory enables us to obtain a unified view of molecular structure at the water surface.

2. RESULTS AND DISCUSSION

At first, we clarify the terminology "ice-like" because this term has been widely used but with different meanings in the past. As mentioned in the Introduction, Shen and co-workers use this term to refer to tetrahedrally coordinated water structures.[8,11,24] Some other researchers used the term just to refer to water in a symmetric environment[31−33] or simply stronger H-bonded water,[34] in a more or less nonattributive way. In this paper, we take Shen's original definition that refers to tetrahedrally coordinated water. Since our question is how the water surface differs from that in the bulk, we regard the structure of the bulk liquid as a reference. Bulk water is believed to consist mainly of (distorted) tetrahedrally coordinated water structures, either as part of a continuum or as a distinct state.[5,35] Therefore, the ice-like interfacial water structure, hereafter, means the water interface showing a tetrahedral structure less distorted than in the bulk and/or increase of the (distorted) tetrahedral component compared with the bulk.

Figure 1 shows the OH stretch region of Im$\chi^{(2)}$ spectra of the air/water interfaces experimentally obtained with various H_2O/HOD/D_2O concentrations (blue, neat H_2O; dark yellow, H_2O:HOD:D_2O = 2:5:3; red, 1:6:9). Within the errors of their and our experiments, our Im$\chi^{(2)}$ spectra are in good agreement with those reported by Tian and Shen,[24] showing a positive band at 3100 cm^{-1} (OH(x)), broad negative OH band(s) around 3200−3600 cm^{-1}, and a sharp positive "free OH" band at 3700 cm^{-1}. The broad OH band in the H_2O spectrum (blue line) consists of a major band around 3450 cm^{-1} (OH(II)) and a weak band at 3250 cm^{-1} (OH(I)). The shoulder at 3620 cm^{-1} is less prominent in the present spectra than that reported by Tian and Shen.[24] As clearly seen in Figure 1, the OH(I) and OH(II) bands merge into one band (OH(0), red line) as H_2O is replaced by HOD (red line). This is a clear evidence of the presence of the vibrational coupling in the H_2O Im$\chi^{(2)}$ spectrum. The loss of the OH(I) (or narrowing of the negative OH band, see Figure 2c for comparison) upon isotopic dilution can also be seen in ref 24. Presumably due to interference between peaks and/or the nonresonant background, the OH(I) band appears more pronounced in the $|\chi^{(2)}|^2$ spectrum (see Supporting Information (SI)). In any case, these results confirm that both $|\chi^{(2)}|^2$ and Im$\chi^{(2)}$ spectra of the neat H_2O surface are affected by intramolecular coupling, as previously pointed out in ref 13, although a possible contribution from intermolecular coupling (delocalization of the vibrational mode) cannot be excluded from the data. Another critical observation is the existence of the positive OH(x) band for all the deuterium concentrations. Because it appears in the isotopically diluted water, the OH(x) band is not due to the intramolecular coupling or collective (delocalized) vibrations via the intermolecular coupling.[27] The low-frequency OH(x) band indicates the presence of water molecules having strong H-bonds.

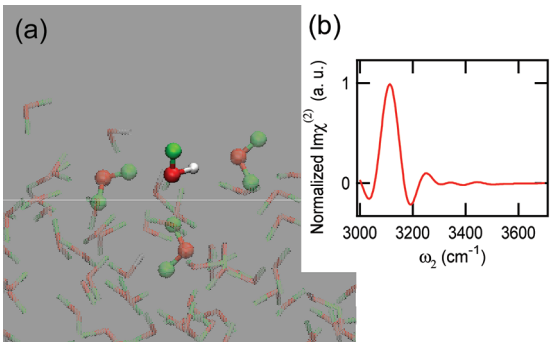

Figure 3. (a) Snapshot in the MD simulation trajectory of the HOD/D_2O mixture, showing the water pair at the surface. Only four water molecules within a 3.25 Å radius, including the HOD at the center, are represented by ball and stick, and the others are represented by sticks only. White, green, and red represent H, D, and O atoms, respectively. (b) The simulated Im$\chi^{(2)}$ spectrum of the four water molecules around the center in the snapshot (a).

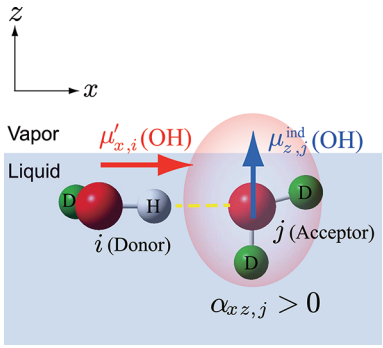

Figure 4. Schematic picture of the isotopically diluted water surface. The left HOD molecule, having a dipole moment in the horizontal plane ($\mu'_{x,i}$(OH)), creates a local field at the OH stretching frequency, resulting in the positive induced dipole moment at the OH stretching frequency ($\mu^{Ind}_{z,j}$(OH)) in the neighboring "D_2O" molecule at the right. The bold dashed yellow line indicates the strong H-bond between these molecules.

To deduce the Im$\chi^{(2)}$ spectra of pure HOD species for direct comparison with MD simulation, we examined the linearity of the concentration-dependent change of the Im$\chi^{(2)}$ spectra (see SI for detail). The dashed line in Figure 1 shows the linear combination of the Im$\chi^{(2)}$ spectra of the water with the highest and lowest deuterium concentrations. The weight of each spectrum was determined by the composition (H_2O:HOD:D_2O = 2:5:3), leaving no adjustable parameters. The resulting dashed line is indistinguishable from the experimental spectrum of the same composition (dark yellow curve), indicating that the spectral change observed in the Im$\chi^{(2)}$ spectrum linearly reflects the isotope concentrations. This linearity allows us to obtain the Im$\chi^{(2)}$ spectrum of the pure HOD from the spectra obtained experimentally, similar to ref 24.

Figure 2a,b shows the intensity-normalized Im$\chi^{(2)}$ spectra of the pure HOD species deduced from the experiment and MD simulation, respectively. In the MD simulations, the isotope ratio was fixed at H_2O:HOD:D_2O = 0:10:90. Apart from the relative magnitude of the free OH band, the simulated Im$\chi^{(2)}$ spectrum in the H-bonded OH region reproduces most features of the experimental spectrum, including the presence of the OH(x) band, zero-crossing frequencies, peak positions, bandwidth of the OH(0) band, and the relative amplitude of the OH(x) and OH(0) bands. (Note that the experimental data contain significant noise below 3100 cm^{-1} due to the weak IR intensity in this region.) This demonstrates that the present MD simulation can reproduce very well the experimental spectrum of HOD in the H-bonded OH region, for which intra-/intermolecular couplings do not play a role.

The experimentally observed H_2O spectrum (Figure 2c) shows considerable broadening of the negative OH band compared to the HOD spectrum, as represented by the shaded area. The theoretically simulated H_2O spectrum (Figure 2d), on the other hand, shows only slight broadening and shift of the negative OH band compared to the simulated HOD spectrum. The larger broadening for the H_2O spectrum observed in the experiment can be attributed to the intramolecular anharmonic coupling, i.e., Fermi resonance, because the anharmonic coupling is not properly included in the classical MD simulation. We note that the experiment did not show significant contribution of the intermolecular coupling, as indicated by the linear dependence of the Im$\chi^{(2)}$ spectra on the isotope concentration, although a detailed analysis of the MD simulation indicated its contribution is not completely negligible. A quantitative analysis of intra- versus intermolecular coupling based on the MD simulation will be discussed elsewhere.

The excellent agreement between the experimental and theoretical Im$\chi^{(2)}$ spectra in the H-bonded OH stretch region for the HOD/D_2O system proves high reliability of the H-bond structure at the water surface provided by the MD simulation. The structure of the HOD/D_2O mixture surface obtained from the MD simulation is completely analogous to that of the pure H_2O surface previously proposed.[29,30] The molecular structure at the water surface is highly mobile and dynamic, and there are no hexagonal H-bonded clusters (see MD simulation video). The H-bonded OH groups near the surface, on average, point down to the bulk, causing the negative OH(0) band at a frequency similar to that of bulk water (~3410 cm^{-1}). The water species that gives rise to the positive low-frequency OH band (OH(x)) is found to be the HOD molecule at the top surface which specifically interacts with a neighboring D_2O molecule (Figure 3a). This is clearly illustrated by the calculated Im$\chi^{(2)}$ spectrum of the water molecules within 3.25 Å around the HOD molecule located around the center of the snapshot. This spectrum displays a positive OH band at a very low frequency (Figure 3b). Note that the OH stretch band is solely due to the HOD molecule at the center because the other water molecules within this radius are D_2O. This clarifies that the OH(x) band does not originate from tetrahedrally coordinated water molecules existing in or below the second layer.[8,11,16,24] The HOD molecule, which gives rise to the positive Im$\chi^{(2)}$ signal, has a OH group lying nearly horizontal and induces positive polarization in the H-bonded neighboring D_2O through the anisotropic local field (Figure 4), as previously suggested for the air/H_2O interface.[28−30] The low OH stretch frequency indicates that the HOD molecule is strongly H-bonded to the neighboring D_2O. Therefore, the positive sign of the OH(x) band is not related to the upward orientation of individual water molecules but to the net response of the dimer. In this mechanism, the frequency of the signal (OH(x) band) depends only on the local O−H bond that creates the local field at the adjacent molecule. For this reason, the intensity of the OH(x) band is linear with the

dx.doi.org/10.1021/ja2053754 |J. Am. Chem. Soc. 2011, 133, 16875–16880

Table 1. Band Assignment of Im$\chi^{(2)}$ Spectra of the Neat Water Surface

OH(x)	strong H-bond pair, appearing through anisotropic local field effect
OH(0)	liquid (uncoupled)
OH(I)	liquid (coupled): the lower frequency component of the Fermi split OH band
OH(II)	liquid (coupled): the higher frequency component of the Fermi split OH band

isotope concentration, and the mechanism of the intermolecular correlation is not mitigated by isotopic dilution.

The present study shows that the water molecules responsible for the OH(x) band are not tetrahedrally coordinated water but are rather undercoordinated. This is consistent with the former gas-phase cluster studies which suggested that three-fold-coordinated water molecules can display a lower OH frequency than four-fold-coordinated water.[36−38] The absence of the ice-like structure at the liquid water surface is in agreement with earlier theoretical studies[39,40] as well as thermodynamical considerations of "surface premelting" at an ice surface. There is ample evidence that the ice surface melts at a temperature lower than the melting point of the bulk ice, i.e., below 0 °C, which is known as surface premelting.[41−45] Even simple thermodynamics denies the presence of the hexagonal ice structure at the surface above the melting point because the entropy gain of melting is always preferable to the enthalpy of the crystallization at any temperature higher than the melting point. Thus, we can conclude that the structure of the air/water interface is not the particular ice-like structure. Table 1 summarizes the assignment of the different OH bands appearing in the Im$\chi^{(2)}$ spectra of H_2O and HOD surfaces, resulting from the combined experimental and theoretical efforts presented here.

Although we can exclude tetrahedrally coordinated "ice-like" water, it is noteworthy that the MD simulation suggests the existence of a strong H-bond at the neat water surface. Recently, the Tahara group reported the Im$\chi^{(2)}$ spectra of isotopically diluted water at charged surfactant/aqueous interfaces.[19,20] The Im$\chi^{(2)}$ spectra do not show the OH(x) band, and the observed OH band is almost identical to the IR spectrum of bulk HOD, indicating that the surface electric field does not enhance H-bonding. The presence of the OH(x) band and the existence of the stronger H-bonds at the neat water surface demonstrate that the water structure at the hydrophobic air/water interface is substantially different from that at hydrophilic charged surfactant interfaces.

After this manuscript was submitted, a Communication about a theoretical study on the air/water interface by the Skinner group appeared.[46] They claimed that the OH(x) band could emerge in their MD calculation with a newly developed three-body potential, which alters the surface structure to emphasize 4D (four-coordinated) water. We found, on the other hand, that current water models widely established for liquid simulations naturally reproduce the OH(x) band if we precisely describe the strong H-bonding interaction. This issue will be further discussed in detail by some of the authors in a forthcoming paper.

3. CONCLUSIONS

In summary, the Im$\chi^{(2)}$ spectra of HOD surface obtained by the experiment and theory agree very well, including the presence of the characteristic positive OH(x) band. This confirms the validity of the Ishiyama−Morita model to describe the molecular structure at the air/water interface. The MD simulation suggests that there is a strong in-plane H-bond between the molecules at the outermost surface, which gives rise to the OH(x) band, but this is not related to a tetrahedrally coordinated water structure. Therefore, the VSFG spectrum does not indicate the existence of ice-like structure at the neat water surface. Comparison between the experimental and theoretical Im$\chi^{(2)}$ spectra of the H_2O surface with those of HOD also confirms that the major source of the isotope effect on the water $\chi^{(2)}$ spectra can be attributed to the intramolecular anharmonic coupling, i.e., Fermi resonance. This should be kept in mind to make correct interpretations of H_2O $\chi^{(2)}$ spectra.

4. MATERIALS AND METHODS

4.1. Experimental Section. Ultrapure water (Millipore, 18.2 MΩ cm resistivity) and deuterium oxide (NMR grade, 99.9%) were mixed to obtain mixtures of H_2O, HOD, and D_2O at desired concentrations. The optical configuration and Fourier transform analysis of HD-VSFG have been described elsewhere.[18] Briefly, a major part of the output from a regenerative amplifier (Spectra Physics, SpitfireProXP; ∼3.5 W, 1 kHz) was used for excitation of a commercial optical parametric amplifier and a difference frequency generator (Spectra Physics, TOPAS C&DFG1) to generate broadband IR (ω_2, center wavelength 2800 nm, bandwidth ∼400 cm^{-1}). The rest of the regenerative amplifier output was narrowed by a band-pass filter (Optoscience, center wavelength 795 nm, bandwidth 1 nm (15 cm^{-1})) and was used as the visible (ω_1) light for the HD-VSFG measurement. The ω_1 and ω_2 beams were spatially and temporally overlapped on a sample surface with incident angles of 44° and 59°, respectively, to generate the sum frequency (SF) at $\omega_1+\omega_2$. The height of the sample surface was maintained with an accuracy of 1 μm using a displacement sensor. The ω_1, ω_2, and SF beams reflected by the sample surface were refocused by a concave mirror onto a GaAs(110) surface to generate another SF that acted as a local oscillator (LO). The SF pulse from the sample passed through a 2-mm-thick silica plate located between the sample and the concave mirror, which delayed the SF pulse relative to the ω_1 and ω_2 pulses by 3.3 ps. This delay generated the time difference between the SF pulse and the sample and that from the GaAs. The two SF beams were introduced together into a polychromator and then detected by CCD. In the polychromator, the two SF pulses were stretched in time and interfered to generate an interference fringe in the frequency domain.[17] A typical CCD exposure time was 2 min, and each spectrum presented in this paper is an average of ∼100 measurements. The SF, ω_1, and ω_2 beams were s-, s-, and p-polarized, respectively. All spectra were normalized by the interference fringe spectrum obtained from a z-cut quartz and GaAs. In the present HD-VSFG measurement, the LO was generated by the ω_1 and ω_2 beams that were reflected from the sample surface. Thus, the measured $\chi^{(2)}$ spectra are affected by the reflectivity dispersion of the infrared at the water surface ($r(\omega_2)$). Therefore, the present $\chi^{(2)}$ spectra of H_2O and HOD have been corrected by $|r(\omega_2)|$ that was measured at the sample surface. The phase shift due to the reflectivity dispersion was calculated to be insignificant.

4.2. Calculation Method. Details of the theoretical calculation are described elsewhere.[29,30] The physical properties of water used in this model, i.e., the radial distribution functions and surface potential, have been examined previously.[47] Here we briefly summarize the essential points in the present MD methodology. The water model employed in the present study is the flexible and polarizable point dipole model developed by Ishiyama and Morita[48] with slight modification for the damping treatment at a short internuclear distance.[29] The MD simulation was executed in a rectangular simulation cell with dimensions of L_x

$\times L_y \times L_z = 30 \times 30 \times 150$ Å^3 in three-dimensional periodic boundary conditions, in which a water slab is formed parallel to the $x-y$ plane with an average kinetic temperature of 298 K. The simulation cell contains 500 water molecules, in which HOD and D_2O are randomly mixed in the ratio of 1:9. We note that the only difference between HOD and D_2O is the proton mass, and the potential function and parameters including the point dipole are common for HOD and D_2O. The long-range Coulombic interaction is treated with the Ewald summation method for the point dipolar system.[48] The second-order nonlinear susceptibility $\chi^{(2)}$ is calculated with the time correlation function formalism[28]

$$\chi^{(2)}_{xxz} = \frac{i\omega_{IR}}{k_B T}\int_0^{T_c} dt \exp(i\omega_{IR}t)\langle A_{xx}(t)M_z(0)\rangle \quad (1)$$

where A and M are the system polarizability and dipole moment, k_B and T are the Boltzmann constant and temperature, and $\langle\cdots\rangle$ is the statistical average in the classical MD simulation. T_c in eq 1 should be infinity in the ideal situation, while we set T_c = 4.9 ps in the MD calculation of $\chi^{(2)}$.[49] In the isotopically dilute water, the O−H stretching modes become localized and independent. Thus we evaluate the contribution of each O−H vibration to the susceptibility $\chi^{(2)}$ (depicted in Figure 3b) in the following way. At first we define a "cluster" region as the first solvation shell of an arbitrary HOD molecule at the surface region, where the radius of the shell is 3.25 Å. We calculate A and M for the molecules within this shell, where the cluster consists of one core HOD and a few solvating D_2O molecules in most cases (see Figure 3a). In this calculation of the time correlation function in eq 1, T_c is set to 1.25 ps, which is short enough to retain the constituent molecules of the cluster.

■ ASSOCIATED CONTENT

Ⓢ Supporting Information. Real part and modulus square of the experimental $\chi^{(2)}$ spectra, details of the linear combination analysis, and complete ref 5. This material is available free of charge via the Internet at http://pubs.acs.org.

Ⓦ Web Enhanced Feature. A movie showing the MD simulation is available in the online version of this article.

■ AUTHOR INFORMATION

Corresponding Author
tahei@riken.jp; morita@m.tohoku.ac.jp

■ ACKNOWLEDGMENT

This work was financially supported by a Grant-in-Aid for Scientific Research on Priority Area (No. 19056009) from MEXT and Grant-in-Aid for Exploratory Research (No. 22655009) from JSPS. A.M. is grateful to Prof. Asuka Fujii for valuable discussion.

■ REFERENCES

(1) Scherer, J. R. In *Advances in Infrared and Raman Spectroscopy*; Clark, R. J. H., Hester, R. E., Eds.; Heyden: Philadelphia, 1978; Vol. 5, p 149−216.
(2) Scherer, J. R.; Go, M. K.; Kint, S. *J. Phys. Chem.* **1974**, *78*, 1304–1313.
(3) Smith, J. D.; Cappa, C. D.; Wilson, K. R.; Cohen, R. C.; Geissler, P. L.; Saykally, R. J. *Proc. Natl. Acad. Sci. U.S.A.* **2005**, *102*, 14171–14174.
(4) Wernet, P.; Nordlund, D.; Bergmann, U.; Cavalleri, M.; Odelius, M.; Ogasawara, H.; Naslund, L. A.; Hirsch, T. K.; Ojamae, L.; Glatzel, P.; Pettersson, L. G. M.; Nilsson, A. *Science* **2004**, *304*, 995–999.
(5) Huang, C.; et al. *Proc. Natl. Acad. Sci. U.S.A.* **2009**, *106*, 15214–15218.
(6) Skinner, J. L.; Auer, B. M.; Lin, Y.-S.; Rice, S. A *Adv. Chem. Phys.* **2009**, *142*, 59–103.
(7) Du, Q.; Superfine, R.; Freysz, E.; Shen, Y. R. *Phys. Rev. Lett.* **1993**, *70*, 2313–2316.
(8) Shen, Y. R.; Ostroverkhov, V. *Chem. Rev.* **2006**, *106*, 1140–1154.
(9) Gopalakrishnan, S.; Liu, D. F.; Allen, H. C.; Kuo, M.; Shultz, M. J. *Chem. Rev.* **2006**, *106*, 1155–1175.
(10) Gragson, D. E.; Richmond, G. L. *J. Phys. Chem. B* **1998**, *102*, 3847–3861.
(11) Du, Q.; Freysz, E.; Shen, Y. R. *Phys. Rev. Lett.* **1994**, *72*, 238–241.
(12) Du, Q.; Freysz, E.; Shen, Y. R. *Science* **1994**, *264*, 826–828.
(13) Sovago, M.; Campen, R. K.; Wurpel, G. W. H.; Muller, M.; Bakker, H. J.; Bonn, M. *Phys. Rev. Lett.* **2008**, *100*, 173901.
(14) Sovago, M.; Campen, R. K.; Bakker, H. J.; Bonn, M. *Chem. Phys. Lett.* **2009**, *470*, 7–12.
(15) Ji, N.; Ostroverkhov, V.; Chen, C. Y.; Shen, Y. R. *J. Am. Chem. Soc.* **2007**, *129*, 10056–10057.
(16) Ji, N.; Ostroverkhov, V.; Tian, C. S.; Shen, Y. R. *Phys. Rev. Lett.* **2008**, *100*, 096102.
(17) Yamaguchi, S.; Tahara, T. *J. Chem. Phys.* **2008**, *129*, 101102.
(18) Nihonyanagi, S.; Yamaguchi, S.; Tahara, T. *J. Chem. Phys.* **2009**, *130*, 204704.
(19) Nihonyanagi, S.; Yamaguchi, S.; Tahara, T. *J. Am. Chem. Soc.* **2010**, *132*, 6867–6869.
(20) Mondal, J. A.; Nihonyanagi, S.; Yamaguchi, S.; Tahara, T. *J. Am. Chem. Soc.* **2010**, *132*, 10656–10657.
(21) Stiopkin, I. V.; Jayathilake, H. D.; Bordenyuk, A. N.; Benderskii, A. V. *J. Am. Chem. Soc.* **2008**, *130*, 2271–2275.
(22) Stiopkin, I. V.; Weeraman, C.; Pieniazek, P. A.; Shalhout, F. Y.; Skinner, J. L.; Benderskii, A. V. *Nature* **2011**, *474*, 192–195.
(23) Chen, X.; Hua, W.; Huang, Z.; Allen, H. C. *J. Am. Chem. Soc.* **2010**, *132*, 11336–11342.
(24) Tian, C. S.; Shen, Y. R. *J. Am. Chem. Soc.* **2009**, *131*, 2790–2791.
(25) Tian, C. S.; Shen, Y. R. *Chem. Phys. Lett.* **2009**, *470*, 1–6.
(26) Buch, V.; Tarbuck, T.; Richmond, G. L.; Groenzin, H.; Li, I.; Shultz, M. J. *J. Chem. Phys.* **2007**, *127*, 204710.
(27) Auer, B. M.; Skinner, J. L. *J. Chem. Phys.* **2008**, *128*, 224511.
(28) Morita, A.; Ishiyama, T. *Phys. Chem. Chem. Phys.* **2008**, *10*, 5801–5816.
(29) Ishiyama, T.; Morita, A. *J. Chem. Phys.* **2009**, *131*, 244714.
(30) Ishiyama, T.; Morita, A. *J. Phys. Chem. C* **2009**, *113*, 16299–16302.
(31) Richmond, G. L. *Chem. Rev.* **2002**, *102*, 2693–2724.
(32) Gan, W.; Wu, D.; Zhang, Z.; Feng, R.; Wang, H. *J. Chem. Phys.* **2006**, *124*, 114705.
(33) Shultz, M. J.; Baldelli, S.; Schnitzer, C.; Simonelli, D. *J. Phys. Chem. B* **2002**, *106*, 5313–5324.
(34) Tyrode, E.; Johnson, C. M.; Kumpulainen, A.; Rutland, M. W.; Claesson, P. M. *J. Am. Chem. Soc.* **2005**, *127*, 16848–16859.
(35) Eisenberg, D.; Kauzmann, W. *The Structure and Properties of Water*; Oxford University Press: London, 1969.
(36) Steinbach, C.; Andersson, P.; Kazimirski, J. K.; Buck, U.; Buch, V.; Beu, T. A. *J. Phys. Chem. A* **2004**, *108*, 6165–6174.
(37) Lenz, A.; Ojamae, L. *J. Phys. Chem. A* **2006**, *110*, 13388–13393.
(38) Mizuse, K.; Mikami, N.; Fujii, A. *Angew. Chem., Int. Ed.* **2010**, *49*, 10119–10122.
(39) Wilson, M. A.; Pohorille, A.; Pratt, L. R. *J. Phys. Chem.* **1987**, *91*, 4873–4878.
(40) Pratt, L. R.; Pohorille, A. *Chem. Rev.* **2002**, *102*, 2671–2691.
(41) Furukawa, Y.; Yamamoto, M.; Kuroda, T. *J. Cryst. Growth* **1987**, *82*, 665–677.
(42) Kouchi, A.; Furukawa, Y.; Kuroda, T. *J. Phys. (Paris)* **1987**, *48*, 675–677.
(43) Lied, A.; Dosch, H.; Bilgram, J. H. *Phys. Rev. Lett.* **1994**, *72*, 3554–3557.

(44) Wei, X.; Miranda, P. B.; Shen, Y. R. *Phys. Rev. Lett.* **2001**, *86*, 1554–1557.
(45) Sazaki, G.; Zepeda, S.; Nakatsubo, S.; Yokoyama, E.; Furukawa, Y. *Proc. Natl. Acad. Sci. U.S.A.* **2010**, *107*, 19702–19707.
(46) Pieniazek, P. A.; Tainter, C. J.; Skinner, J. L. *J. Am. Chem. Soc.* **2011**, *133*, 10360–10363.
(47) Ishiyama, T.; Morita, A. *J. Phys. Chem. C* **2007**, *111*, 721–737.
(48) Ishiyama, T.; Morita, A. *J. Phys. Chem. C* **2007**, *111*, 738–748.
(49) Morita, A. *J. Phys. Chem. B* **2006**, *110*, 3158–3163.